Measurement and statistical analyses of fission and fusion excitation functions for ^{35}Cl on ^{62}Ni, ^{116}Sn, and ^{141}Pr up to $E_{lab}=215$ MeV

B. Sikora
The Institute of Experimental Physics, Department of Nuclear Physics, Warsaw University, Warsaw, Poland

W. Scobel
Institut für Strahlen und Kern Physik, Bonn University, Bonn, Federal Republic of Germany

M. Beckerman
Laboratory for Nuclear Science, Massachusetts Institute of Technology, Cambridge, Massachusetts

J. Bisplinghoff
Institut für Strahlen und Kern Physik, Bonn University, Bonn, Federal Republic of Germany

M. Blann
E-Division, Lawrence Livermore National Laboratory, Livermore, California 94550
(Received 20 July 1981; revised manuscript received 29 September 1981)

Evaporation residue and fission-like cross sections are reported for the bombardment of ^{62}Ni, ^{116}Sn, and ^{141}Pr targets with 200 and 215 MeV ^{35}Cl ions. These data plus data previously reported at lower energies have been analyzed by a Hauser-Feshbach statistical code with Bohr-Wheeler model fission competition. The rotating liquid drop model was used to evaluate effective fission barriers. Barrier reductions of 35–45 % of the rotating liquid drop model values were required over an angular momentum range for which fission was measured, in agreement with earlier analyses. The sensitivity of results to the sharp cutoff assumption was tested and found to be unimportant over the energy ranges covered in this work.

[NUCLEAR REACTIONS Measured $\sigma_{ER,f}$ ^{35}Cl+^{62}Ni,^{116}Sn,^{141}Pr $E_{lab}=200$, 215 MeV. Deduced statistical fission parameters.]

I. INTRODUCTION

In the statistical/rotating liquid drop (SRLD) model the transition state approach of Bohr and Wheeler[1] is combined with the rotating liquid drop model as formulated by Cohen, Plasil, and Swiatecki.[2] The fission barrier heights decrease with increasing angular momentum, and the fission widths become functions of angular momentum as well as excitation energy. For medium mass systems, such as those considered in this work, the nonrotating fission barriers are high, and the SRLD model predicts that fission originates predominantly from high spin states in highly deformed nuclei.

We will test the SRLD model description of high spin state deexcitation by comparing predicted and experimental cross sections for fission and evaporation residue formation. For this purpose experimental data are necessary which extend to excitation energies where fission favorably competes with evaporation residue (ER) formation. We have therefore performed experiments to obtain additional results on fission and ER formation following ^{35}Cl bombardment of ^{58}Ni, ^{116}Sn, and ^{141}Pr at laboratory energies of 200 and 215 MeV, respectively. These results extend earlier measurements which were made at energies up to 170 MeV.[3,4]

This extended data set will be analyzed using a Hauser-Feshbach statistical model code.[5] Multiple chance fission/particle emission calculations will be performed with explicit angular momentum coupling between initial and final states in the continuum; experimentally deduced J_{cr} values will be used to generate the initial population of states. We will employ statistical fission parameters deduced previously[6] from analyses of fission and evaporation residue excitation functions in the fission threshold region; we shall demonstrate the influence of small parameter variations, but no gross parameter adjustment search is made.

We will then reanalyze the excitation functions using a second, more self-consistent SRLD para-

metrization to obtain more precise information on those single particle and collective properties of highly deformed nuclei represented by the statistical fission parameters. Finally, we will examine the sensitivity of the results to the use of the sharp cut-off approximation.

II. EXPERIMENTAL PROCEDURE AND RESULTS

A. Measurements

Experiments were performed at the Brookhaven National Laboratory Van de Graaff facility in a three-stage operation. The ^{62}Ni and ^{116}Sn targets were self-supporting and of 100 and 175 μg/cm^2 thickness, respectively; the ^{141}Pr target was 200 μg/cm^2 thick and on a 20 μg/cm^2 carbon backing. Heavy reaction products were measured with counter telescopes, consisting of a ΔE gas counter and a (E-ΔE) solid state detector. The experiment was monitored by two solid state detectors mounted symmetrically with respect to the projectile beam axis. The detector angle thus was defined to better than $\pm 0.2°$. Evaporation residue data were taken between $\sim 3°$ and 15° (lab) in 1° or 2° steps; data for fission fragments were measured up to c.m. angles well beyond 90°. The absolute differential cross sections were obtained by normalization of monitors and telescopes via Rutherford scattering. The experimental procedures have previously been described in detail.[7] A typical spectrum of this work is shown in Fig. 1 as a contour diagram.

B. Experimental results

Angular distributions of the evaporation residue products are presented in Fig. 2; angular distributions of fission and fission-like fragments in the c.m. system have been obtained by assuming (i) binary fission with Z/A being equal to that of the primary reaction system; (ii) kinetic energies of the fragments as given by Viola's formula[8]; and (iii) neglect of particle evaporation. Integration over masses has been performed centering around the region of symmetric division which was well separated from projectile or target-like fragments for the ^{116}Sn and ^{141}Pr targets. The resulting angular distributions are shown in Fig. 3. They seem to follow a $1/\sin\theta_{\text{c.m.}}$ distribution which therefore has been taken as the basis of determining the angle-integrated fission cross sections σ_f.

A special word of precaution applies to ^{35}Cl + ^{62}Ni leading to a reaction system with a fissility

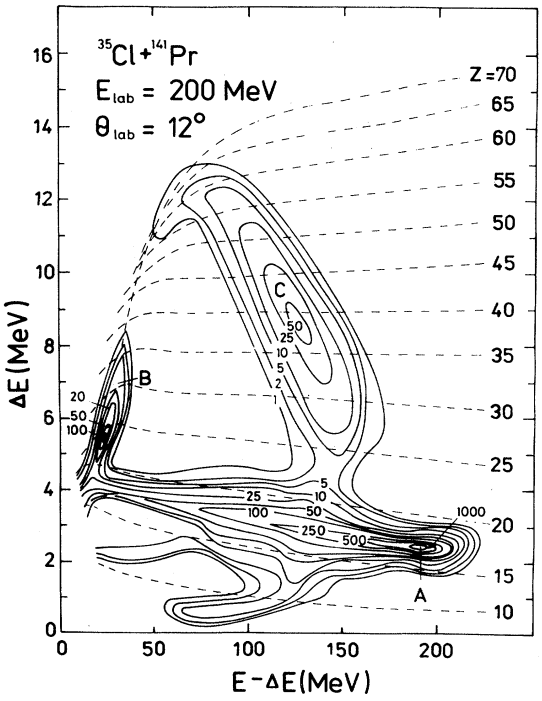

FIG. 1. Contour diagram E vs (E-ΔE) for 200 MeV ^{35}Cl on ^{141}Pr at θ lab = 12°. The region A represents elastically scattered ^{35}Cl, B represents evaporation residues, and C represents the fission fragment region.

parameter $x = 0.41$. While the fission-like product angular distributions are fitted by a $1/\sin\theta$ curve satisfactorily (see Fig. 4), the charge yield distributions are unusually broad (Fig. 5), even at the lower bombarding energies,[3] and show some asymmetry about target and projectile charge. The fission-like yields probably contain major fractions of deep inelastic yields, making a statistical analysis ambiguous. Nonetheless, as the yields may be from equilibrium fission, it is worth analyzing results in terms of the model to be presented. We have therefore integrated the charge yield only at higher angles and extrapolated by means of a $1/\sin\theta$ distribution to obtain σ_f.

Integrated evaporation residue and fission cross sections are given in Table I, where results at lower bombarding energies are also presented.[3,4] Experimental uncertainties are indicated for each result presented.

III. STATISTICAL MODEL ANALYSES OF FISSION AND FISSION-LIKE EXCITATION FUNCTIONS

Fission and/or evaporation residue excitation functions have frequently been analyzed using a

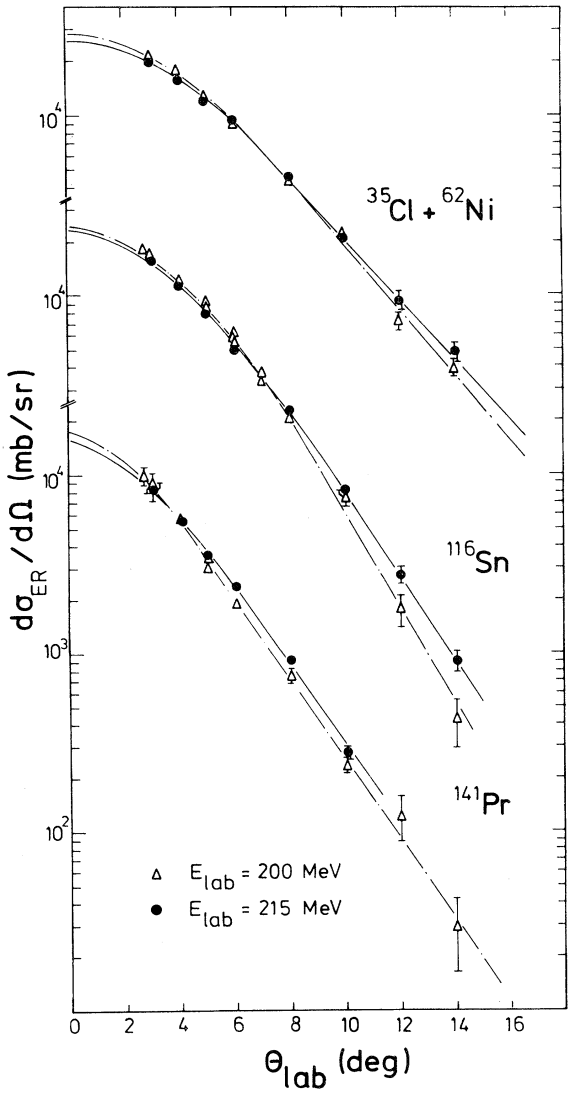

FIG. 2. Evaporation residue angular distributions for ^{35}Cl bombardment of ^{62}Ni, ^{116}Sn, and ^{141}Pr targets. Open triangles represent results at 200 MeV (lab) ^{35}Cl energy, closed circles represent yields at 215 MeV. The lines were arbitrarily drawn through the points and were used for integrating the angular distributions.

Hauser-Feshbach (HF) statistical model for light particle emission with a Bohr-Wheeler transition state model[9–11] for predicting the rate of fission deexcitation. For the latter, for nuclei at high angular momenta, the rotating liquid drop model (RLDM) of Cohen *et al.*[2] has been used as a starting point to provide ground state and saddle point energies necessary for the calculations. All uncertainties have been forced into two parameters in

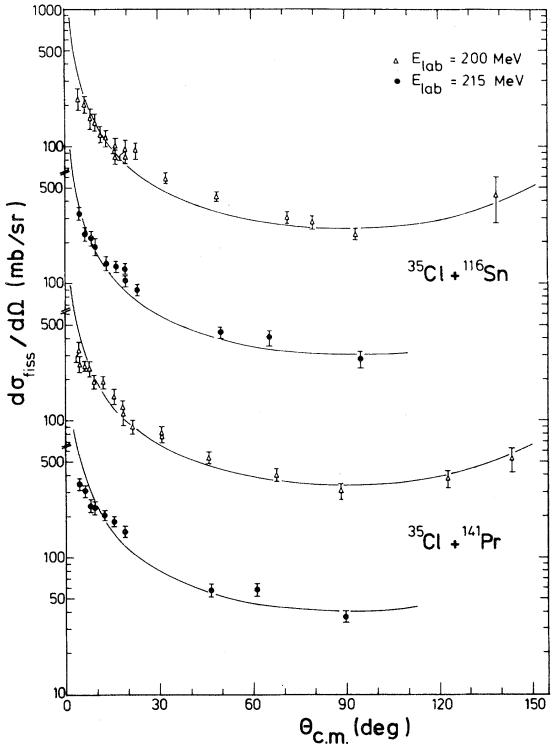

FIG. 3. Fission fragment angular distributions for fission or fission-like fragments following 200 and 215 MeV ^{35}Cl bombardment of ^{116}Sn and ^{141}Pr targets. Solid curves are normalized $1/\sin\theta$ functions.

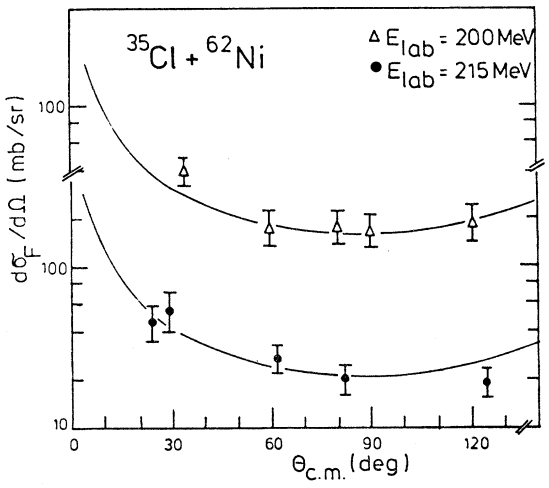

FIG. 4. Angular distribution for fission/fission-like fragments following 200 and 215 MeV ^{35}Cl bombardment of ^{62}Ni. The solid curves are normalized $1/\sin\theta$ functions.

these analyses.[9–13] One is the assumed ratio of single-particle level densities at the saddle point to that of the rotating ground state, a_f/a_ν. The other is the height of the angular momentum dependent fission barrier. The latter has most frequently been treated by scaling the angular-momentum-dependent liquid drop fission barrier [represented herein as $B(I)$] by a constant B_f. Some discussion has recently been presented to indicate that both B_f and a_f/a_ν should be considered functions of angular momentum, if analyses are not expected to give physically significant parameters as results.[14] We shall give a short presentation of the HF model applied and the parametrization chosen and then discuss the calculations in context with our experimental data.

A. The model

The SRLD fission width Γ_f and particle emission width Γ_ν are specified as functions of excitation energy E and angular momentum I by[6,11]

$$\Gamma_f(E,I) \propto (2I+1) \int_0^{E-E_{\rm sp}(I)} \rho_f[E-E_{\rm sp}(I)-k]dk \tag{1}$$

and

$$\Gamma_\nu(E,I) \propto (2S_\nu+1) \sum_{l=0}^{\infty} \sum_{J=|I-l|}^{I+l} \int_0^{E-E_{\rm min}(J)-B_\nu} \rho_\nu[E-E_{\rm min}(J)-B_\nu-\epsilon]T_\nu^l(\epsilon)d\epsilon \ , \tag{2}$$

where J denotes the residual nucleus angular momenta. The quantities $E_{\rm sp}$ and $E_{\rm min}$ denote the rotational energies of the saddle point deformed nucleus and the equilibrium deformed nucleus, respectively; their difference is the I-dependent fission barrier $B(I)$:

$$E_{\rm sp}(I)=E_{\rm min}(I)+B(I) \ . \tag{3}$$

Following Bohr and Wheeler, k denotes the fission mode degree of freedom, the transmission coefficients above the barrier are assumed to be unity and those below the barrier are assumed to be zero. The level densities used are of the form $\rho_i(U) \propto U^{-2}\exp 2(a_i U)^{1/2}$ with excitation energies U decremented by the appropriate rotational energies, and with $a_\nu=A/10$, throughout. In Eq. (2), S_ν denotes the intrinsic spin of particle ν, ϵ its channel energy, and B_ν its binding energy. The transmission coefficients $T_\nu^l(\epsilon)$ at orbital angular momenta l are computed using the nuclear optical model as described previously.[6,11]

The initial, compound nucleus spin populations $\sigma(\epsilon,I)$ are obtained by means of the sharp-cutoff approximation from the measured complete fusion cross sections $\sigma_{\rm CF}(\epsilon)$:

$$\sigma(\epsilon,I)=\begin{cases} \pi\lambda\!\!\!^{-2}(\epsilon)\cdot(2I+1), & I \le l_{\rm cr}(\epsilon) \ , \\ 0 \ , & I > l_{\rm cr}(\epsilon) \ , \end{cases} \tag{4}$$

with

$$\sigma_{\rm CF}(\epsilon)=\pi\lambda\!\!\!^{-2}(\epsilon)[l_{\rm cr}(\epsilon)+1]^2 \ , \tag{5}$$

where $\lambda\!\!\!^{-}$ denotes the reduced deBroglie wavelength of the incident ion.

The excitation functions are described in terms of the two free statistical fission parameters a_f/a_ν and B_f; the former denotes the ratio of single-particle level densities at the saddle point to those at equilibrium deformation, and the latter denotes a scale factor for the RLD fission barriers:

$$B(I)B_f=E_{\rm sp}(I)-E_{\rm min}(I) \ , \tag{6}$$

i.e., the I dependence of B is fully taken from the RLD model. The decay of the subsequent excited evaporation residues is treated the same way; the population is followed for $\Delta E=1$ MeV and $\Delta I=1$ $\hbar$ bins.

Parameter values found previously[6] from analyses of fission threshold excitation functions (155 to 170 MeV) listed in Table II have been used to test the SRLD model at higher bombarding energies, where fission competition limits ER formation. These parameters a_f/a_ν and B_f should be looked upon as representing average values over the angular momentum windows contributing to fission. It should be repeated that there is absolutely no justification for extrapolating parameters determined over a limited but high angular momentum range to zero angular momentum, and further that noncompound contributions to the experimental cross sections, or inadequacies of the statistical model formulation or input parameters are forced to be reflected in the a_f/a_ν and B_f parameters by analyses of this type.

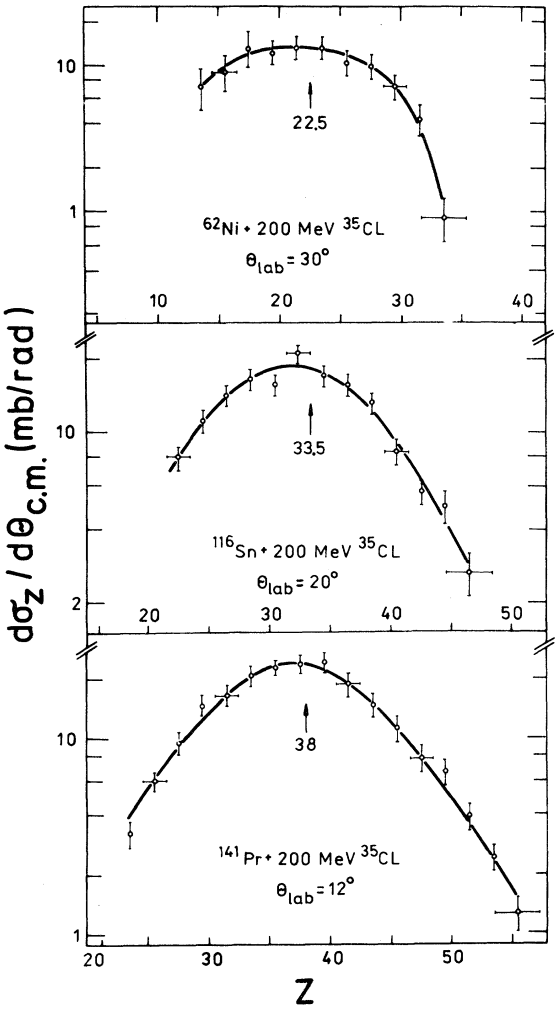

FIG. 5. Z distributions for 200 MeV ^{35}Cl on ^{62}Ni, ^{116}Sn, and ^{141}Pr. Solid curves have been drawn as a visual guide.

The second set of SRLD parameters are angular momentum dependent[15] and explicitly reflect RLD shape changes. We take

$$\Delta(I)=0,\ (a_f/a_\nu)(I)=1 \text{ for } I>I_2;$$
$$\Delta(I)=\Delta_0,\ (a_f/a_\nu)(I)=(a_f/a_\nu)_0 \quad (6)$$

for $I<I_1$, and we linearly interpolate at intermediate angular momenta. The energy shifts $\Delta(I)$ are related to the rotational energies by

$$B(I)-\Delta(I)=E_{sp}(I)-E_{min}(I)\ . \quad (7)$$

The quantities I_1 and I_2 are listed in Table II; I_2 denotes the angular momenta at which the saddle point and equilibrium deformations coincide. I_1 represents the approximate angular momentum at which fission first begins to be significant; we do not probe the barrier values at lower I with the data reported in this work.

1. Sensitivity of parameters to direct fission/deep inelastic reaction admixture

There are a great many questions which must be answered before parameters extracted by analyses of the type under discussion are interpreted in terms of the angular momentum dependent fission barrier heights and the single particle level densities—rather than only as effective parameters which allow data to be reproduced, as we interpret them. This point is addressed in subsection III C.

One point which can be addressed is the uncertainty in fission excitation function analyses caused by other than equilibrium fission contributions to

TABLE I. Summary of experimental results including those (marked with asterisk) of Ref. 3.

Reaction	ϵ_{lab} (MeV)	155*	160*	165*	170*	200	215
^{35}Cl + ^{62}Ni	σ_{ER} (mb)		998±70	1089±76	1091±76	960±70	956±70
	σ_f	45±9	78±15	114±22	126±24	340±100	420±85
	σ_{CF}		1076±72	1203±80	1217±80	1300±120	1376±110
	l_{cr} ($\hbar$)	59	60	64	66	74	79
^{35}Cl + ^{116}Sn	σ_{ER}		446±31		560±39	586±41	583±41
	σ_f	15±2	37±6	79±12	135±45	500±75	600±90
	σ_{CF}		493±31		695±59	1086±85	1183±99
	l_{cr} ($\hbar$)	43	48	54	60	81	88
^{35}Cl + ^{141}Pr	σ_{ER}	96±17	132±15	179±18	253±25	270±40	279±42
	σ_f	19±4	70±10	135±20	180±40	670±70	800±120
	σ_{CF}	115±17	203±18	314±27	433±47	940±80	1079±127
	l_{cr} ($\hbar$)	24	32	41	49	79	88

TABLE II. Statistical fission parameters applied in this work.

System	a_f/a_ν	B_f	$(a_f/a_\nu)_0$	Δ_0 (MeV)	$I_1(\hbar)$	$I_2(\hbar)$
$^{35}Cl + {}^{62}Ni$	1.04	0.54	1.07	10.0	40	81
$^{35}Cl + {}^{116}Sn$	1.02	0.57	1.07	8.20	35	76
$^{35}Cl + {}^{141}Pr$	1.03	0.65	1.05	5.00	30	74

the measured fission-like cross sections. These contributions have been referred to as direct fission, and/or deep inelastic reactions. Direct fission may be defined as reactions proceeding by a path in which the fusing system passes inside the conditional (one dimensional) saddle point determined by the frozen entrance channel asymmetry, with reseparation of the fragments before passing inside the true compound nucleus saddle point.[16] Deep inelastic events may be defined as strongly damped reactions which do not pass within the conditional saddle point.[16] There is not a unanimity in these definitions, which we will use in this work. What is clear is that there may be mechanisms other than equilibrium fission contributing to experimentally measured fission-like yields, and proven models to divide the measured results between the possible modes await future development. We will refer to evaporation residue (σ_{ER}), compound nucleus fission (σ_f), direct fission (σ_{DF}), and deep inelastic (σ_{DI}) cross sections in the following discussion.

At the lower bombarding energies the major portion of the fusion/fission-like cross section is found (for the composite Z systems which we have investigated) in evaporation residue products. Clearly the compound nucleus trajectory prevails. As the bombarding energy is increased, a two body decay (fission like) rapidly increases in the cross section. Two possibilities exist: (1) The higher partial waves just beyond the evaporation residue survival values redivide by equilibrium fission, perhaps with still higher partial waves going into either or both of the noncompound binary decay modes broadly defined above; or (2) only noncompound binary decay modes compete with evaporation residue formation.

In the second case above, it is clear that parameters of the type extracted in this work are only that, and cannot be interpreted in terms of fission barrier heights and single particle level densities. While this could be the case and we do not rule it out, it is quite unlikely. Rather (1) seems a more reasonable situation (which is a necessary but not sufficient condition for a literal interpretation of extracted parameters). The question which must be addressed when tentatively accepting (1) is the impact of the uncertainty in dividing the fission-like cross sections between compound and noncompound contributions upon the parameters extraeted. This is a point which merits discussion.

This situation is schematically illustrated in Fig. 6, where a hypothetical division of cross sections due to the different mechanisms is shown. For simplicity in the preliminary discussion, sharp divisions in the ultimate fate of entrance channel angular momenta are shown. Various entrance channel angular momenta (l) are shown in Fig. 6, corresponding to values which would be deduced from $\sigma_{ER}(l_1)$, or from the ER plus fission cross sections (l_2), etc.

Assume that we somehow knew the exact ER and compound nucleus fission cross sections. Then an evaporation/fission statistical decay calculation would be performed, varying parameters until the measured cross sections for σ_{ER} and σ_f were reproduced. This really means that the parameters are varied until all partial waves above l_1 are predicted to undergo fission, and all those of value l_1 or lower are predicted to survive fission.

Next assume that while the evaporation residue cross section could be measured accurately, it was

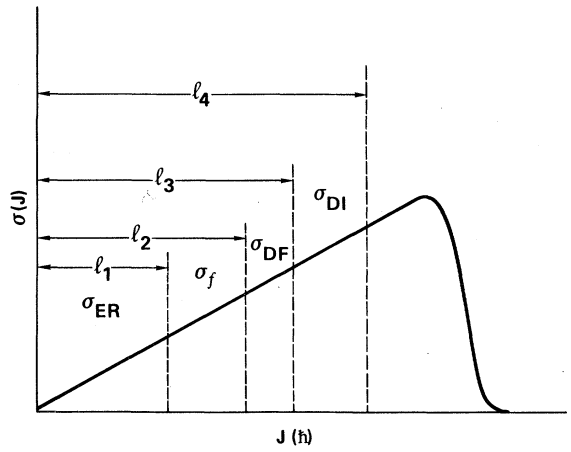

FIG. 6. Schematic diagram of the division of the reaction cross section into compound and noncompound portions. This figure is discussed in subsection III A 1.

impossible to separate σ_f from σ_{DF} and σ_{DI}. Then the evaporation/fission calculation would be performed assuming that all partial waves up to l_4 were in the compound nucleus distribution; however, the resulting calculated fission cross section would be compared not with σ_f (experimental), but with $\sigma_f+\sigma_{DF}+\sigma_{DI}$ (experimental). Agreement would be equivalent to the statement that all partial waves between l_4 and l_1 were predicted to undergo fission, or in other words the parameter set is that which results in ER survival for partial waves l_1 or less, fission for waves greater than l_1. This is exactly the same set as determined for the case that the σ_f could be measured free of any contamination from other binary decay processes. The determination of parameter sets may then be seen to be independent of the ability to separate the various binary decay mode cross sections, *if the l_1 division results from equilibrium fission competition.*

Next, one can question how this conclusion changes if the sharp-cutoff assumption is removed. If the higher partial waves which undergo equilibrium fission go predominately into fission, the conclusion is unchanged.

So much for the hypothetical world. The real world involves uncertainties in experimental results. This means that σ_{ER} and therefore the limiting angular momenta for ER production or survival have uncertainties. Similarly the values for fission-like cross sections have uncertainties. Parameter fitting in general must realistically consider the degree to which the compound nucleus uncertainty modifies calculated fission cross sections. This is particularly true when $\sigma_f << \sigma_{ER}$, for in this region σ_f is changing very rapidly with the assumed compound nucleus angular momentum. Similarly in this region, where only a *fraction* of each of the highest partial waves is estimated to undergo fission (so that the l_{ER} limit has not yet saturated due to fission competition), the problem of separating equilibrium from nonequilibrium fission contributions may introduce considerable uncertainty into the interpretation of statistical fission parameters. In the present work, it is unlikely that this situation is encountered for the Sn and Pr target systems; the Ni system is open to question until such time as data permitting separation of a clear symmetric fission component become available. However, we emphasize the point above: When evaporation residue survival is limited by equilibrium fission competition, parameters extracted should not depend upon separation of equilibrium and nonequilibrium components. There are, however, many very important questions which must be addressed and answered before the statistical parameters extracted from such analyses may be interpreted as physically meaningful quantities, and many of these points are addressed in subsection III C.

B. Results

Fission and ER excitation functions have been calculated using the code MBII (Ref. 5) to evaluate Eqs. (1)–(8) with level density parameters $a_\nu = A/10\ \mathrm{MeV}^{-1}$.

1. *Parametrization with B_f and a_f/a_ν*

The individual channel fission excitation functions for the three systems under investigation are shown in Figs. 7 and 8. For ^{35}Cl and ^{116}Sn calculations have been performed with the full RLD fission barriers (i.e., $B_f=1$); they are not able to reproduce the fission onset, whereas the SRLD calculation with the "best" parameters of Table II with reduced fission barrier ($B_f=0.54-0.65$) and a_f slightly (2–4 %) enhanced over a_ν reproduces both the shapes and relative magnitudes of the fission

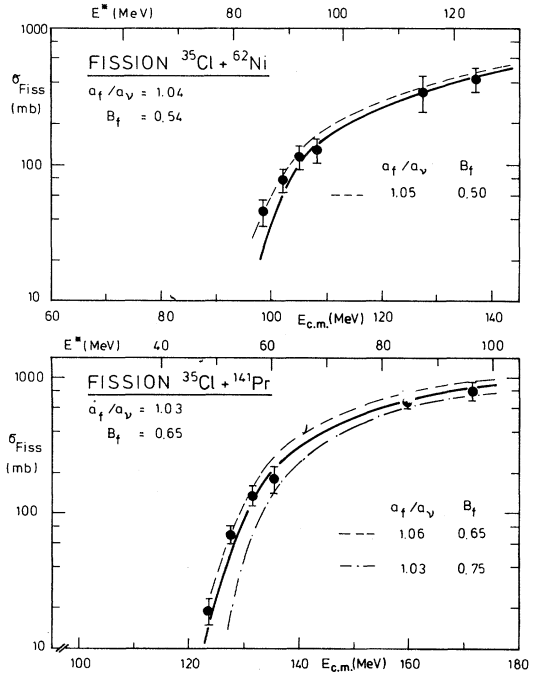

FIG. 7. Calculated and experimental fission excitation functions for ^{35}Cl + ^{62}Ni and ^{141}Sn. Calculations are discussed in the text.

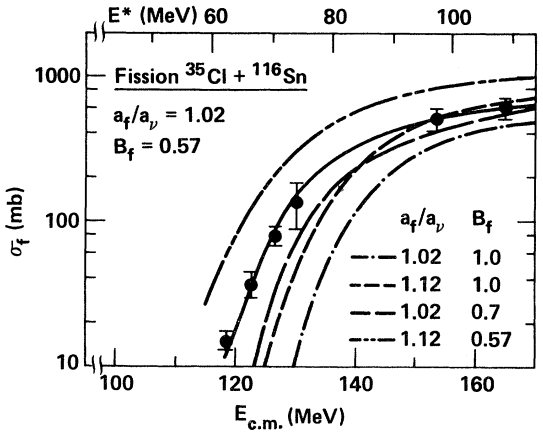

FIG. 8. Calculated and experimental fission excitation functions for $^{35}Cl + ^{116}Sn$. Calculations are discussed in the text.

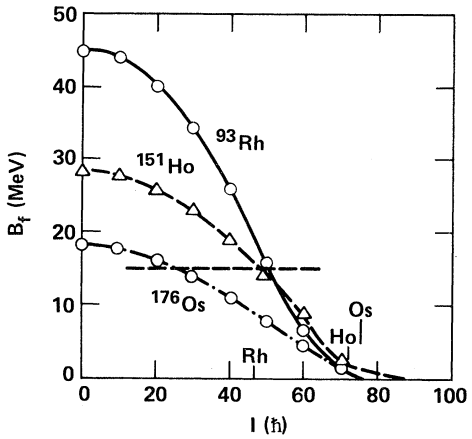

FIG. 9. Rotating liquid drop model fission barriers for ^{93}Rh, ^{151}Ho, and ^{176}Os versus angular momentum. The angular momenta at which the RLDM predicts each nucleus to change from an oblate to a prolate ground state shape is indicated on the abscissa by the elemental chemical symbol.

and thus also the ER excitation functions. In particular, the model correctly gives the leveling of the ER cross sections at high projectile energy.

Fission excitation functions calculated with other parameter sets have also been investigated and results are presented in Figs. 7 and 8. It may be seen that there is some latitude in choice of parameters which will fit the experimental excitation functions; however, all require a substantial ($\geq 30\%$) reduction of the RLD fission barriers over the angular momentum ranges for which fission contributions are significant. These are the angular momenta for which $B(I)$ varies from $\approx 8-15$ MeV. The predicted RLDM barriers versus angular momentum for the systems studied in this work are indicated in Fig. 9. The effect of the parameter B_f is that it decreases the fission barrier $B(I)$ in a way that it becomes comparable with the neutron separation energy S_n when the angular momenta I approach the l_{cr} for energies at the onset of fission.

The decrease of the fission barrier implies that for high energies, e.g., $^{35}Cl + ^{116}Sn$, ^{141}Pr, and $E_{Cl} \geq 200$ MeV, first chance fission dominates whereas for lower energies (or the low angular momenta) multiple chance fission is important and may even dominate, cf. Figs. 10–12.

There is a question as to sensitivity of the parameters extracted to the sharp cutoff approximation used for deducing the limiting angular momentum for fusion l_{cr}. This point was investigated for the case of the ^{116}Sn target by replacing the sharp cutoff by one having a linear cutoff over $\Delta l = 6\hbar$ centered about l_{cr}. All calculated fission cross sections between 150 and 215 MeV were within 2% of those using the sharp cutoff model, illustrating that the SCO approximation introduced no significant uncertainty over the $E-I$ range relevant in this work. This is not the case at lower energies where Γ_f/Γ_{tot} is a steeper function of I.

It is of interest to compare the parameter a_f/a_ν predicted by a simple model for a Fermi gas in a deformed potential with the values empirically deduced in this work. Values calculated for a_f and a_ν based on the formula of Bishop *et al.*[17] are present-

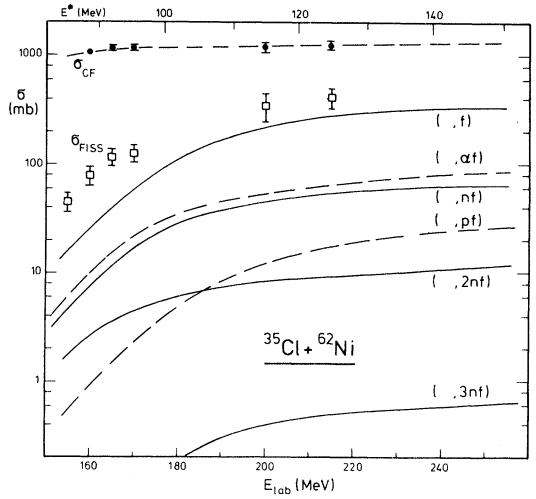

FIG. 10. Fission channel excitation functions for $^{35}Cl + ^{62}Ni$ reactions. Solid curves are calculated by MBII code for various channels using the "best" parameter sets given in Table I. Experimental fission (open squares) and complete fusion (closed circles) results are also shown.

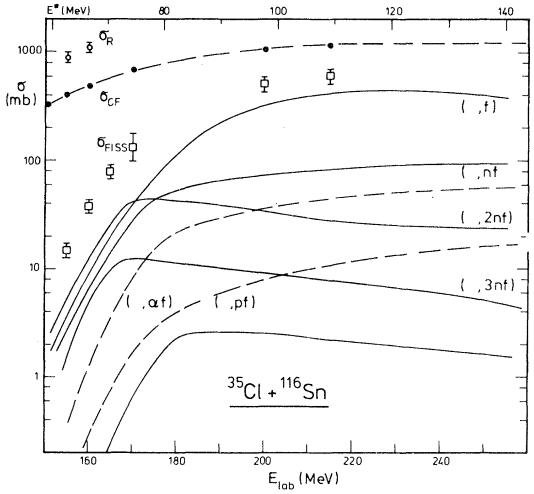

FIG. 11. As in Fig. 9 for ^{116}Sn targets.

ed in Fig. 13. The model predicts

$$a_{\nu,f}=[(33+4/\Delta_R+8\Delta_R^{1/2})/45]a_0\ , \qquad (8)$$

where

$$\Delta_R=\left[\frac{R\,\text{major}}{R\,\text{minor}}\right]^{2/3}$$

and R major (R minor) is the major (minor) axis of the deformed nucleus and a_0 is the single particle level density for the spherical nucleus. Values used in Eq. (8) for preparation of Fig. 13 were taken from the RLD model. We have limited saddle point shapes to ellipsoids of revolution in evaluating R minor. It may be seen that the a_f/a_ν ratios predicted by the simple model of Bishop are in excellent agreement with those deduced by fitting the data. The fission barrier (B_f) parameters, one should remember, correspond to some average over the fission window range of angular momenta; they represent barrier height reductions of $\approx$5 MeV or less (cf. also Ref. 18).

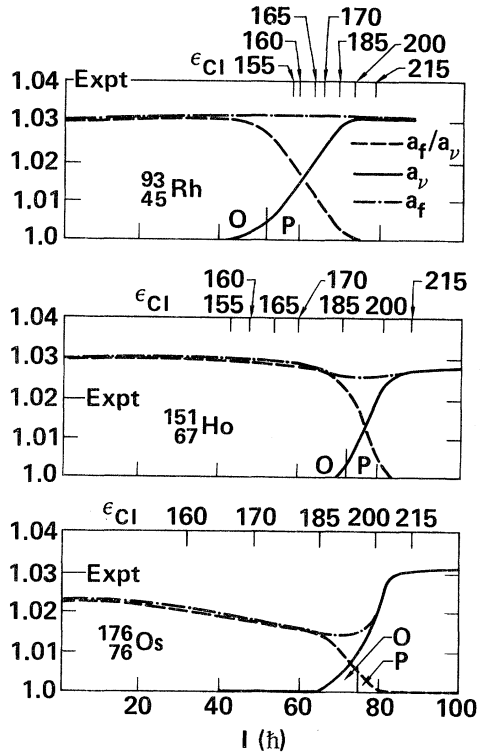

FIG. 13. Single particle level density parameters versus angular momentum for deformed nuclei. Results are computed using deformations from RLDM with the formula of Bishop *et al.* (Ref. 17). Results are shown for the ground state deformations (a_ν, solid line), for the saddle point deformations (a_f, dotted line), and for the ratio a_f/a_ν (dashed line). The maximum angular momentum deduced for each bombarding energy is shown above each set of results. The RLDM angular momenta at which shape transitions between oblate (o) and prolate (p) are expected are indicated on the abscissas.

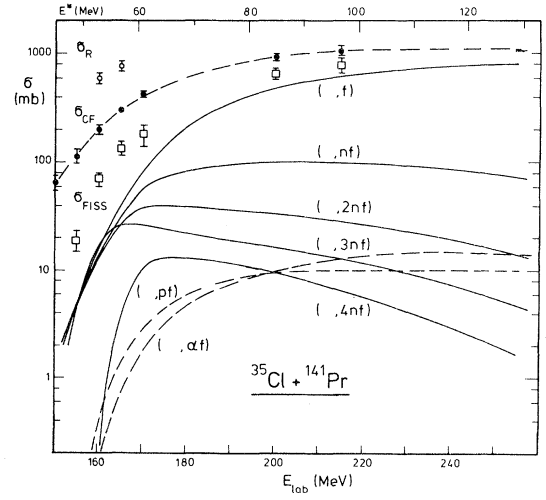

FIG. 12. As in Fig. 9 for ^{141}Pr targets.

From this agreement it may be inferred that the RLD description is at least qualitatively correct. Some of the measured l_{cr} values do exceed those for which the RLD fission barriers vanish; these latter quantities (I_2) are listed in Table II. However, the vanishing of the fission barrier does not preclude deformation enhanced particle emission[19] which may well stabilize nuclei at high angular momenta. More likely, the highest partial waves are resulting from a "direct fission" mechanism. This, however,

would not affect the validity of the extracted parameters as long as some range of partial waves exists for equilibrium fission between the highest partial wave for ER production and the lowest partial wave for direct fission, as discussed in subsection III A 1.

2. *Parametrization with $\Delta_0(I)$ and a_f/a_ν*

Values for $(a_f/a_\nu)_0$ and Δ_0 obtained from refitting the fission and evaporation residue excitation functions over the entire measured energy range and reproducing them equally well, as in Figs. 7 and 8, are presented in Table II. The values for $(a_f/a_\nu)_0$ are slightly higher than those for a_f/a_ν. These ratios are consistent with predictions based on differences in the amount of nuclear surface relative to the interior between saddle point and equilibrium deformed nuclei.[11,16] Similar single particle level density ratios have been obtained from analyses of light ion induced fission measurements for systems of similar fissilities.[20]

The energy shifts Δ_0 range from 10.0 to 5.0 MeV; the corresponding saddle point energies $E_{sp}(I_1)$ range from 55 to 19 MeV. These reductions are substantial, although at least part of the decreases may be due to the neglect of the finite range in the RLD model. Liquid drop calculations performed with a finite range[21,22] give lower point energies than do those of Ref. 2. Other possibilities were discussed in Ref. 11.

Additional results of SRLD analyses of recent fission threshold cross section measurements[21] for the ^{40}Ca + ^{62}Ni system are presented in Table III. The first set of $(a_f/a_\nu)_0$, Δ_0 values yield the same cross sections as those obtained using $a_f/a_\nu=1.03$, $B_f=0.54$.[6] These cross sections are less than the experimental ones by roughly the same amount as found for the ^{35}Cl + ^{62}Ni system.

To examine the sensitivity of the deduced parameters to the use of the sharp cutoff approximation, the above-mentioned calculations were repeated using a linear taper to σ_{CF} of $8\hbar$ width (the same as the taper width to the calculated total reaction cross section). The result shown in Table III is that the calculated fission cross section at 160 MeV is increased by $\sim$25%. The calculated increases in σ_f are not significant when compared to those resulting from small changes in statistical fission parameters. This point is illustrated by the last set of SRLD calculations performed with Δ_0 increased by 10% to 12.8 MeV. The resulting increases in σ_f are greater than those obtained from the angular momentum taper, and are sufficient to bring the calculations into agreement with the measurements.

C. Comparisons of parameter sets with results of other works

There may appear to be discrepancies between parameter sets deduced in this work and in other works, and there are surely philosophic differences as to how literally these parameter sets should be interpreted.

One point of view *vis-a-vis* heavy ion data of the type shown herein is that there is question as to the reaction mechanisms and therefore of application of statistical theory to these heavy ion systems.[11] Further, it has been pointed out that the older statistical formulations may be in need of modification for systems at the very high excitations and angular momenta encountered in heavy ion reactions, and due to these uncertainties, extracted parameters should be considered as effective parameters until it is demonstrated that the analyses are valid.[11,19] It was further emphasized that the fission barriers are only probed in such experiments where the heights are (broadly) in the range of 8–12 MeV.[11] One simple approach out of many possibilities is to scale the RLD barriers by a constant. It has been emphasized that there is no justification whatever in extrapolating barrier scaling parameters determined

TABLE III. Calculated and experimental fission cross sections for Ca + Ni.

$(a_f/a_\nu)_0$	Δ_0 (MeV)	σ_f (160 MeV) (mb)	σ_f (170 MeV) (mb)	Cutoff width ($\hbar$)
1.07	11.6	5.7	26.0	0
1.07	11.6	7.1	31.0	8
1.07	12.8	12.0	44.0	8
		20 ± 10[a] expt.	60 ± 20[a] expt.	

[a]Reference 23.

in this manner at, e.g., $60-70\hbar$ to zero angular momentum, and indeed illustrations have been given of other methods of changing the RLD barriers which give equally good fits to data with totally different implications for barriers at zero angular momenta.[15] In these works, covering systems from $A=97$ to $A=176$, effective barrier height parameters ranging from 54% to 70% of the RLD results were found over the energy ranges of measurement, as confirmed also in this work.

A philosophically opposite point of view is contained in a recent work by Plasil *et al.*,[13] who measured fission excitation functions and (at three energies for each system) evaporation residue cross sections for $^{20}Ne + {}^{133}Cs$ and $^{12}C + {}^{141}Pr$. They fitted their fission excitation functions over the range of measurement (considerably lower angular momenta than the results of this work) with parameters $a_f/a_\nu=1.08$, $B_f=0.83$, where B_f multiplies the RLD barriers at all angular momenta. From these results they concluded first that the fission barriers at zero angular momenta are indeed 0.83 times the liquid drop model result, and second that other parameter sets must be in error, even though those sets were determined for systems of different masses and angular momenta. Thus the two extremes of interpretation exist.

Still another result, due to Karwowski and Vigdor,[24] should be mentioned; they measured fusion/fission excitation functions and fission angular distributions for $^{197}Au + {}^{6}Li$ reactions. They found that no reduction of the RLD fission barriers was necessary to reproduce their experimental results. This might seem a further inconsistency; however, this is not necessarily the case. One should tender judgement by considering the physics involved and the degrees of freedom. The RLD model is, by the standards we are applying in barrier extraction, a crude formulation which sacrifices accuracy in order to achieve a general, guiding global predictive capability for nuclei at very high angular momenta. Thus it uses nuclei with sharp surfaces, giving up influences on barriers due to finite range effects,[21,22] and those due to diffuse surface effects on the moment of inertia (important for rotating systems), and of course shell structure influences.[25] It might therefore be expected to show systematic errors in predicted fission barriers at zero angular momenta with A, Z of the compound nucleus due, e.g., to neglect of the finite range effect, and with angular momentum due to inadequate parametrization of the moment of inertia. Comparison of different experimental results must clearly consider these degrees of freedom in the expected behavior of the fission barriers versus a liquid drop model reference surface.

Consider the finite range correction first suggested by Krappe and Nix and more recently refined by Krappe, Sierk, and Nix.[21,22] Figures 10 and 12 of Ref. 21 show that the liquid drop barrier should need little or no adjustment at masses above $A=200$ due to the finite range effect. This is consistent with the conclusion of Karwowski and Vigdor (who studied an $A\approx200$ system).[24] The finite range correction (at zero angular momentum) is expected to increase with decreasing Z^2/A or mass number. Around mass 150 the finite range effect predicts a barrier lower than the liquid drop barrier by ≈7 MeV or 25% (Fig. 12, Ref. 21, for the case that surface parameters are normalized to reproduce the same ^{236}U fission barrier in liquid drop and finite range models) and around mass 96 the barrier is lower by 14.5 MeV or $\approx30\%$. It can be seen in this case that the finite range effect predicts that the $J=0$ fission barriers should have a mass-dependent discrepancy with respect to the liquid drop reference surface. The result of Karwowski and Vigdor is not in this perspective in any disagreement with barriers for lower mass systems which are deduced to be less than the liquid drop barriers as suggested by parameter sets of the present work, or by those of Plasil *et al.* (if a literal interpretation is placed on the parameter sets). However, the Plasil results for $Z=65$ compound nuclei seem quantitatively different than results for the $Z=67$ system deduced in the present work. We must consider expectations of barrier height scaling versus angular momentum in order to compare the work of Plasil[13] with the present work, and also differences which may be code dependent and unrelated to physics. Finally we should consider the correspondence between the parameters deduced and the actual barriers, or the difficulties involved in taking that last (giant) step in interpretation.

The rotating drop model has not as yet been treated with inclusion of finite range and surface diffuseness effects in a sufficiently extensive manor to quote *vis-a-vis* corrections to the angular momentum dependence of the liquid drop reference barrier. However, to first order we would expect the zero angular momentum correction to persist over a fairly broad range of angular momenta. In Fig. 14 (upper) we show the rotating liquid drop fission barrier versus angular momentum for ^{153}Tb. Below it, barriers with finite range corrections of 3.4 and 7 MeV based on two sets of results from Ref. 21 are

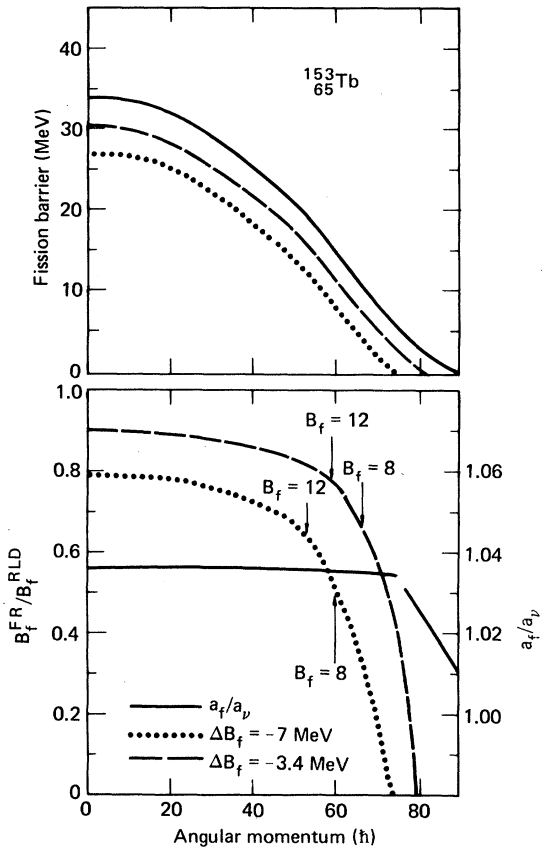

FIG. 14. Statistical fission parameters versus angular momentum for ^{153}Tb. The upper set of curves represents the RLD model predicted fission barrier versus J (solid line). The dashed and dotted curves have constant decrements of 3.4 and 7 MeV representing 10% and 20% reductions from the $J=0$ barriers. The lower curves show the ratio of the decremented barrier heights (B_{fFR}) to the RLD model barriers versus J for the 10% and 20% reduction factors. Angular momenta are indicated at which the modified fission barriers are 8 and 12 MeV, the approximate window of sensitivity for fitting data. The Fermi gas prediction of a_f/a_ν according to the prescription used in Ref. 17 is given as a solid curve.

shown.

In the lower portion of Fig. 14 we show the ratio of the angular momentum dependent barriers to the RLD results versus J ($\hbar$) when a constant finite range correction is applied at all angular momenta. The data of Plasil *et al.* involve fitting σ_f of $\lesssim 10$ mb, with the fit weighted to the lowest cross sections, which are of the order 3×10^{-2} mb. The maximum angular momentum involved for these points is approximately $42\hbar$; at this value of the angular momentum the predicted barrier multiplier parameter for the dotted curve of Fig. 14 is ≈ 0.72. For the $Z=67$ (Cl + Sn) system of this work the fission cross sections fitted are weighted towards systems of $J \approx 50\hbar$ or greater. The barrier reduction factor at $50\hbar$, using the 7 MeV finite range reduction factor, would be 0.51. These values of 0.71 and 0.51 may be compared with the corresponding values deduced in Ref. 13 of 0.83 and in this work of 0.57. The trend of differences in barrier multipliers of Ref. 13 and the present work may therefore be explained quite well by consideration of the angular momentum dependence of the corrected fission barriers, if one assumes a constant factor as in the finite range model rather than an arbitrary constant scaling parameter at all angular momenta. It should be noted that these two approaches can give vastly different predictions for the barriers at zero angular momenta. This emphasizes again the danger of arbitrarily extrapolating the high J fission data to obtain zero angular momentum barriers.

Several additional points of caution should perhaps be made concerning the data of Ref. 13 and the parameters extracted therein. The fission cross sections are in the Z region where $\Gamma_f/\Gamma_t \ll 1$, for which analyses will be very dependent on separating equilibrium fission from other binary decay processes. Secondly, results in this region are highly sensitive to both the assumed sharp cutoff distribution (whereas results of this work were found to be relatively insensitive as discussed in subsection III B 1) and to the absolute accuracy of the evaporation residue and fission cross sections. The latter were mostly measured only at one angle in Ref. 13, and only three evaporation residue cross sections were measured for each system. Only statistical errors were quoted, with no estimate of absolute uncertainties ($a \pm 2\hbar$ uncertainty corresponds to a factor of 2 change in calculated fission cross sections). Additionally the ^{20}Ne and especially ^{12}C projectiles are known to have considerable tendency to undergo partial fusion (which would easily be included in the fusion cross sections by the methods used), and were at quite high E/A above the Coulomb barrier when compared with the data of the present work. For these reasons it is not clear that one should expect an agreement between parameter sets deduced for the data of Ref. 13 and the present work.

There remains the question of code dependence of parameters extracted, and of questions of physics. The questions of collective enhancement of level densities were exquisitely discussed and explicately considered by Vigdor and Karwowski,[24] who used a version of the MBII code in their analyses. For

their mass system the deformation effects on transmission coefficients are not important, and we concur in their conclusions which they based on very careful analyses of their excellent data (which included additional constraints due to experimental fission fragment angular distributions).

For lighter mass systems the barrier heights deduced from fitting experimental results do seriously depend on the deformation effect on T_l, on the inclusion or neglect of collective enhancement on level densities, and on the modeling used to determine a_f/a_ν. Extensive calculations are currently in progress to assess the uncertainties in parameters due to each of these properties for the systems reported in this work which could influence parameters and their interpretation. For example, Ref. 13 reports a best parameter set for a Weisskopf-Ewing code analysis of the data, of $a_f/a_\nu=1.08$, $B_f=0.83$. This parameter set fails in a Hauser-Feshbach code (MBII), but the set $a_f/a_\nu=1.00$, $B_f=0.70$ is satisfactory. In a new Hauser-Feshbach code in which level densities are treated in a more rigorous fashion, different parameter sets are found, the values depending upon level density types used and T_l sets. We note that less barrier reduction is required in the $A=97$ region in these calculations.

These analyses are largely made practical by new generation computers with array processors. Results are not yet available, but should allow some statement as to barrier heights over given angular momentum ranges with an estimate of the uncertainty due to questions of form of level density used, and of assumed dependence of corrections to the RLDM barriers with angular momenta. In conjunction with these codes it would be extremely valuable to have results of calculations similar to the RLD model, but including finite range and surface diffusivity effects on the moment of inertia. Such work is in progress.[26]

IV. CONCLUSIONS

Fission excitation functions for ^{35}Cl induced reactions on ^{62}Ni, ^{116}Sn, and ^{141}Pr may be reproduced very well by a statistical model (HF) calculation in which the RLDM fission barriers of partial waves predicted to contribute to the fission cross sections have been reduced by 35 to 45%, in agreement with earlier analyses. The a_f/a_ν parameters simultaneously deduced in the fitting process are in excellent agreement with the formula of Bishop *et al.*[16] using the major and minor axes predicted by the RLD model; however, we note that the model predicts an angular momentum dependent a_f/a_ν ratio rather than a constant value. Therefore, a second set of fission barrier and level density parameters reflecting the RLD shape changes in a corresponding linear angular momentum dependency has been used, yielding an equally satisfactory reproduction of the experimental σ_f data.

We have also shown that over the range of energies and angular momenta considered in this work, the SCO approximation should not seriously alter the parameters deduced from statistical analyses. This preliminary consistency of the fission parameters encourages statistical analyses to extract physically meaningful parameters. This should involve calculations in which the a_f/a_ν and B_f parameters have an angular momentum dependence based on nuclear modeling.

[1]N. Bohr and J. A. Wheeler, Phys. Rev. 56, 426 (1939).
[2]S. Cohen, F. Plasil, and W. J. Swiatecki, Ann. Phys. (N.Y.) 82, 557 (1974).
[3]J. Bisplinghoff, P. David, M. Blann, W. Scobel, T. Mayer-Kuckuk, J. Ernst, and A. Mignerey, Phys. Rev. C 17, 177 (1978).
[4]P. David *et al.*, Nucl. Phys. A287, 179 (1977).
[5]M. Beckerman and M. Blann, University of Rochester Report No. UR-NSRL-135A, 1977 (unpublished); M. Blann and T. T. Komoto, Lawrence Livermore National Laboratory report (unpublished).
[6]M. Beckerman and M. Blann, Phys. Lett. 68B, 31 (1977).
[7]H. H. Gutbrod, W. G. Winn, and M. Blann, Nucl. Phys. A213, 267 (1973).
[8]V. E. Viola, Jr., Nucl. Data 1, 391 (1966).
[9]H. Freiesleben, H. C. Britt, and J. R. Huizenge, *Third International Atomic Energy Symposium on Physics and Chemistry of Fission* (IAEA, Vienna, 1974), Vol. I. p. 447.
[10]M. Blann and F. Plasil, Phys. Rev. Lett. 29, 303 (1972); F. Plasil and M. Blann, Phys. Rev. C 11, 508 (1975).
[11]M. Beckerman and M. Blann, Phys. Rev. C 17, 1615 (1978).
[12]J. Bisplinghoff *et al.*, Phys. Rev. C 16, 1058 (1977).
[13]F. Plasil *et al.*, Phys. Rev. Lett. 45, 333 (1980).
[14]M. Blann and J. Bisplinghoff, Lawrence Livermore National Laboratory Report 85886, 1981 (unpublished).
[15]M. Beckerman, Phys. Lett. 78B, 17 (1978).
[16]W. J. Swiatecki, Nucl. Phys. A (to be published).
[17]C. J. Bishop, I. Halpern, R. W. Shaw, Jr., and R. Van-

denbosch, Nucl. Phys. A198, 161 (1972).
[18]J. Barrette, P. Braun-Munzinger, C. K. Gelbke, H. E. Wegner, B. Zeidman, A. Gamp, H. L. Harney, and T. Walcher, Nucl. Phys. A279, 125 (1977).
[19]M. Beckerman and M. Blann, Phys. Rev. Lett. 42, 156 (1979); M. Blann and T. A. Komoto, Phys. Rev. 24, 426 (1981).
[20]L. G. Moretto, S. G. Thompson, J. Routti, and R. C. Gatti, Phys. Lett. 38B, 471 (1972); G. M. Raisbeck and J. W. Cobble, Phys. Rev. 153, 1270 (1967).
[21]H. J. Krappe, J. R. Nix, and A. J. Sierk, Phys. Rev. 20, 992 (1979).
[22]H. J. Krappe and J. R. Nix, in *Proceedings of the Third International Atomic Energy Symposium on Physics and Chemistry of Fission* (IAEA, Vienna, 1974), Vol. I, p. 159.
[23]B. Sikora, M. Blann, J. Bisplinghoff, W. Scobel, and M. Beckerman, Phys. Rev. C 20, 2119 (1979).
[24]H. Karwowski, thesis, Indiana University, 1980 (unpublished); S. E. Vigdor, Nukleonika (to be published).
[25]I. Ragnarsson, T. Bengtsson, G. Leander, and S. Aberg, Lund University Report Lund-MPN-80/07, 1980 (unpublished).